

Tailoring the Spectra of Terahertz Emission from CdTe and ZnTe Electro-Optic Crystals

Minwoo YI, Kang Hee LEE, Inhee MAENG¹, Joo-Hiuk SON¹, R. D. AVERITT², and Jaewook AHN*

Department of Physics, Korea Advanced Institute of Science and Technology, Daejeon 305-701, Korea

¹*Department of Physics, University of Seoul, Seoul 130-743, Korea*

²*Department of Physics, Boston University, Boston, MA 02215, U.S.A.*

(Received September 29, 2007; accepted October 21, 2007; published online January 18, 2008)

We compare the spectral amplitude of terahertz pulses generated using difference-frequency mixing, via the second-order nonlinear process in CdTe and ZnTe, with numerical model calculations using the nonlinear Maxwell equation. We have found that the spectral details of the generated terahertz pulses from CdTe are well explained by considering the effects of optical and terahertz absorptions, diffraction, and the frequency dependence of nonlinear coefficients. This method allows us to design tailored compound materials with improved versatility for generating specific terahertz pulse shapes.

[DOI: [10.1143/JJAP.47.202](https://doi.org/10.1143/JJAP.47.202)]

KEYWORDS: terahertz, pulse shapes, CdTe, ZnTe, zincblende, phase matching

Recent developments in terahertz (THz) science and technology have enabled many potential applications in communications,^{1–4} material characterization,^{5,6} biological and medical imaging,^{7,8} and rotational and vibrational molecular dynamics.^{9,10} Of particular importance has been the development of terahertz time-domain spectroscopy (THz-TDS), allowing robust measurement of the electric field amplitude and phase in a gated fashion obviating the need for bolometric detection. In addition, two-dimensional THz-TDS has resulted in the imaging of biological samples with a view towards simultaneous chemical identification. As a final example, the coherent manipulation of carrier dynamics in semiconductor nanostructures,¹¹ quantum systems such as Rydberg atoms,¹² and Cooper pairing in superconductors¹³ can be investigated using THz pulses. For many of these new applications, the ability to generate THz radiation with a variety of temporal and spectral shapes is required.

Our motivation in this work is to obtain an improved understanding of THz generation process when femtosecond optical pulses impinge on electrooptic crystals. Our emphasis is on determining which factors most strongly affect the resulting spectral amplitude and temporal shape of the generated THz pulses. More specifically, using difference-frequency mixing via the nonresonant second-order nonlinear process in tailored compound materials, it may be possible to improve their versatility for generating specific THz pulse shapes. While the spectral features of THz pulses generated from ZnTe have been widely studied,^{14–16,18} similar studies for CdTe have been rare.¹⁷ Recently, ternary Zn_{1-x}Cd_xTe crystals with various composition ratios x , were studied for the generation of THz pulses using a near-IR optical beam.^{19,20} The generation of THz waves from those crystals was experimentally observed and the optimal composition of $x = 0.05$ for (110)-oriented Zn_{1-x}Cd_xTe was reported.

In this study, we discuss the various factors involved in the generation process of THz beams from CdTe and ZnTe by comparing their spectral amplitudes with results from numerical model calculations. The temporal response and spectral amplitude of THz pulses generated by a difference-frequency mixing process within an ultrafast IR pulse are mainly governed by the momentum mismatch condition between the optical and THz pulses in the nonlinear

medium. The momentum mismatch Δk influences the inverse of the coherence length l_c of the optical rectification process for a material with dispersion at optical frequencies. The coherence length l_c , which depends on the efficiency of THz wave generation, is given by

$$l_c(\Omega; \lambda_{\text{opt}}) = \frac{\pi}{\Delta k} = \frac{\pi c}{\Omega |N_{\text{eff}}(\lambda_{\text{opt}}) - n_{\text{THz}}(\Omega)|}, \quad (1)$$

where $N_{\text{eff}}(\lambda_{\text{opt}})$ is the effective refractive index for an optical pump beam with a wavelength of λ_{opt} ,²¹

$$N_{\text{eff}}(\lambda_{\text{opt}}) = n_{\text{opt}}(\lambda_{\text{opt}}) - \lambda_{\text{opt}} \left. \frac{dn_{\text{opt}}(\lambda)}{d\lambda} \right|_{\lambda_{\text{opt}}}, \quad (2)$$

and $n_{\text{THz}}(\Omega)$ is the index of refraction for the generated THz waves with a frequency of Ω .

If we consider an electric field of ultrafast IR pulses with laser bandwidths of more than 2 or 3 THz, a terahertz wave can be generated as a result of difference-frequency generation among all the pairs of the frequency components within each pump pulse in a second-order nonlinear medium. The amplitude of each spectral component of the local THz field $E^{\text{THz}}(\Omega, z)$ is computed by solving the nonlinear Maxwell equation in the spatiotemporal Fourier domain:²²

$$\frac{\partial^2}{\partial z^2} E^{\text{THz}}(\Omega, z) + \varepsilon(\Omega) \frac{\Omega^2}{c^2} E^{\text{THz}}(\Omega, z) \quad (3)$$

$$= - \frac{4\pi\Omega^2}{c^2} P(\Omega, z), \quad (4)$$

where the polarization $P(\Omega, z)$ is the product of the second-order nonlinear susceptibility $\chi^{(2)}(\Omega)$ and the Fourier components of the intensity of the pump laser pulse:

$$P(\Omega, z) = \chi^{(2)}(\Omega) I(\Omega) \exp\left(\frac{i\Omega z}{v_g}\right). \quad (5)$$

Here, v_g is the group velocity of the optical pulse, and if the pump laser pulse is assumed to be Gaussian with width τ_{opt} , the Fourier component of the intensity of the pump laser pulse may be expressed as $I(\Omega) = I_0 \exp[-(\tau_{\text{opt}}\Omega)^2/2]$.

The solution for this nonlinear Maxwell equation is obtained at each point in the crystal as¹⁸

$$E^{\text{THz}}(\Omega, z) \propto \Omega^2 \chi^{(2)}(\Omega) I(\Omega) z \text{sinc}\left(\frac{\Delta k z}{2}\right). \quad (6)$$

The frequency dependence of the second-order nonlinear coefficient, $\chi^{(2)}(\Omega)$, in the THz frequency region is applied

*E-mail address: jwahn@kaist.ac.kr

using the phenomenological Miller's relation.²³⁾ The dominant change of $\chi^{(2)}(\Omega)$ is due to the frequency dependence of the index of refraction in the THz frequency region, which is obtained from refs. 24 and 25. The effects of optical and THz absorption

$$I(z) = I_0 \exp(-\alpha_{\text{opt}}z), \quad (7)$$

and

$$E^{\text{THz}} \propto \exp[-\alpha_{\text{THz}}(l-z)/2], \quad (8)$$

can be substituted into eq. (6). In our experimental setup, the beam size of the generated THz wave is comparable to the wavelength at a THz frequency, and we need to consider the effect of diffraction. As a function of the diffraction angle of the THz wave, the electric field amplitude becomes²⁶⁾

$$E(\theta) \propto \frac{J_1(k_{\text{THz}}a \sin \theta)}{k_{\text{THz}}a \sin \theta}, \quad (9)$$

where a is the spot size and k_{THz} is the momentum at the THz frequency. We note that the phase-matching term in eq. (6) needs to be slightly modified as well, but in our experiment the change turns out to be negligible.

The experiments for generating and detecting THz radiation are carried out using ~ 90 fs near-IR pulses from a mode-locked Ti:sapphire laser with an 82 MHz repetition rate generating an average power of 750 mW. The temporal shape of the laser is assumed to be Gaussian, with a pulse width of 90 fs. The laser was modulated at 2 kHz using a mechanical chopper to enable lock-in detection. The pump beam was polarized at 55° to the z -axis of the $\langle 110 \rangle$ zincblende crystals in order to maximize the THz radiation.²⁷⁾ The THz transient field generated via optical rectification in the zincblende crystals was collimated and then focused onto a photoconductive switch by two off-axis parabolic mirrors. The spectral amplitude of the THz field generated in 2-mm-thick ZnTe for various center wavelengths (760, 800, and 850 nm) is displayed in Fig. 1(b).

The optical and far-IR refractive indexes of ZnTe may be obtained from the Sellmeier equation²⁸⁾ and the phonon oscillation model,²⁴⁾ respectively. The results of these calculations for 2-mm-thick ZnTe are displayed in Figs. 1(a) and 1(c). Below the pump wavelength of 780 nm, for the 2-mm-thick crystal, two different regions of the THz spectrum satisfy the phase-matching condition, resulting in the bifurcation of the generated THz spectrum. The phase-matched region of the THz spectra generated from a given crystal thickness of ZnTe bifurcates into two parts, and the location of spectral split depends on the center wavelength of the near-IR femtosecond pump beam used for optical rectification, as shown in Fig. 1(a). When the pump laser pulse is tuned below 760 nm, some of the low-frequency parts of the THz pulse are phase matched below the crystal thickness; thus, these low-frequency components do not pass through the 2-mm-thick emitter crystal. As the center wavelength of the pump laser pulse increases, the relative spectral amplitude of the lower THz frequencies increases and the spectral width of the generated THz pulse expands. As expected, the THz spectral width becomes broader when the excitation pulse is around 800 nm. The reason for this is that in the vicinity of 800 nm, the optical and far-IR refractive indices result in optimal phase matching. How-

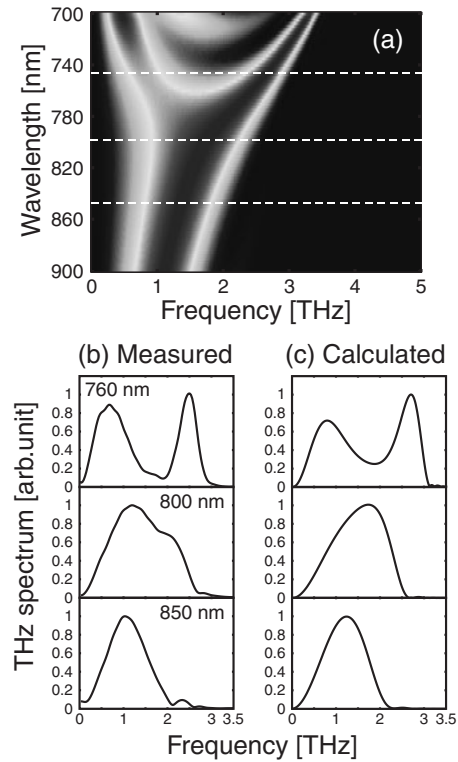


Fig. 1. (a) Spectral bifurcation of generated terahertz waves from a 2-mm-thick ZnTe crystal, shown as a function of the pump laser wavelength. The calculation was performed using a nonlinear Maxwell equation for the difference-frequency mixing process with the additional optical effects described in the text. (b) Measured terahertz spectrums for three different pump laser wavelengths: 760, 800, and 850 nm. For comparison, the model calculations under similar experimental conditions are shown in (c).

ever, for center wavelengths longer than 800 nm, the spectral width of the generated THz field narrows and the peak response of the THz radiation is red-shifted to lower frequencies. The results are comparable to the experimentally measured spectral amplitudes generated with pulses having similar center wavelengths.

By changing the crystal thickness at a fixed pump laser wavelength for the process of THz generation, another spectral bifurcation can be found. Figure 2 shows the calculated spectral amplitude of the THz radiation as a function of the crystal thickness. The wavelength of the pump laser is assumed to be tuned in such a way that the THz spectral bifurcation appears between the thicknesses of the two given ZnTe crystals. As the crystal thickness increases, the frequencies from 1.0–2.0 THz are reduced in amplitude compared with the lower and higher frequencies. This is consistent with the experimental results presented in Fig. 2(c) and can be accounted for by the above discussion of Fig. 1.

The computed THz spectra of CdTe are compared with measured results in Fig. 3. The amplitudes of the measured THz spectrums in $\langle 110 \rangle$ CdTe crystals with two different crystal thicknesses of 200 and 400 μm are shown in Fig. 3(b). The pump laser was tuned at 780 nm. The refractive indexes of CdTe may be obtained from refs. 25 and 28. The experiment was performed above the energy band gap, where our experimental sample thicknesses, 200 and 400 μm , become appropriate for the measured total absorption length of 181 μm of our sample. Although the absorption length of CdTe at the pump laser frequency is

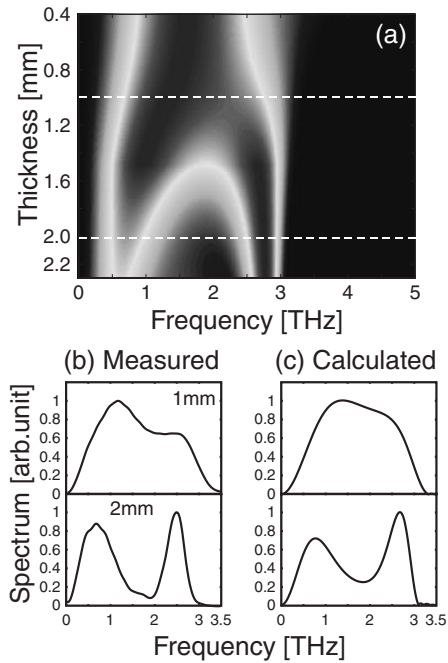


Fig. 2. (a) Spectral shift and distortion due to the rapid change of the phase-matching condition presented as a function of the crystal thickness. (b) Measured spectra of generated terahertz waves from 1- and 2-mm-thick crystals pumped by a laser tuned at 760 nm. (c) Model calculations for similar experiments.

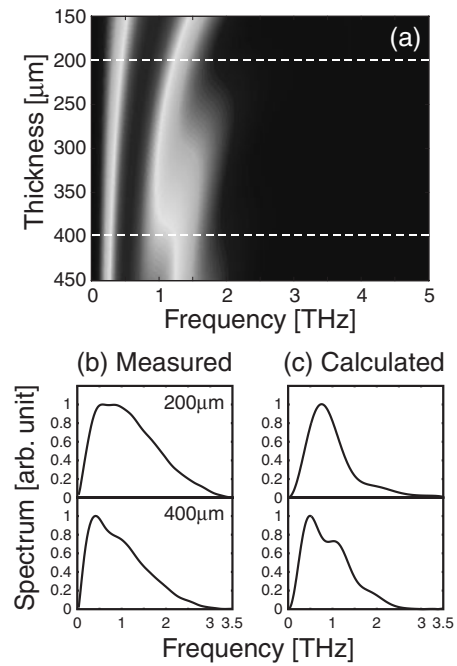


Fig. 3. (a) Model calculation of terahertz spectrum from a CdTe emitter with varied thickness, illuminated by a pump laser at the wavelength of 780 nm. (b) Measured and (c) calculated spectra for the two different crystal thickness of 200 and 400 μm .

significant, because the laser used in the experiment has a large bandwidth, a significant spectral portion of the optical pulse travels the entire crystal thickness. The coherence length for phase matching between a 0.5 THz wave and an optical pulse is 213 μm ; therefore, phase matching is satisfied for our 200 μm sample but not for the 400 μm sample. As the optical absorption gradually plays a larger role in determining the spectrum, the phase-matching condition is shown as a gentle frequency shift as a function of thickness, as shown in Fig. 3(a), and the result is consistent with the measured results in Fig. 3(b).

In summary, we have investigated the spectral amplitude of THz pulses generated from (110) ZnTe and CdTe zincblende crystals. When the generated THz pulses travel through the crystals, spectral shaping is primarily governed by the coherence length of the crystal. We have also found that the effects of optical and THz absorptions, diffraction, and the frequency dependence of nonlinear coefficients become important for fully discussing spectral details. The numerical analysis used for model calculations may be extended to the consideration of other bi- and ternary zincblende crystals such as ZnS, GaP, $\text{ZnSe}_x\text{Te}_{1-x}$, $\text{Zn}_{1-x}\text{Cd}_x\text{Se}$, and $\text{Zn}_{1-x}\text{Mg}_x\text{Te}$ when the frequency component of the pump laser pulse and the crystal properties are varied.

This research was supported by MOEHRD Grant KRF 2005-205-C00024 from the Korea Research Foundation.

- 1) D. S. Citrin and S. Hughes: *Appl. Phys. Lett.* **78** (2001) 1805.
- 2) T. Kleine-Ostmann, P. Dawson, K. Pierz, G. Hein, and M. Koch: *Appl. Phys. Lett.* **84** (2004) 3555.
- 3) N. Krumbholz, K. Gerlach, F. Rutz, M. Koch, R. Piesiewicz, T. Kurner, and D. M. Mittleman: *Appl. Phys. Lett.* **88** (2006) 202905.
- 4) J. J. Simpson, A. Taflove, J. A. Mix, and H. Heck: *IEEE Microwave Wireless Components Lett.* **14** (2004) 343.
- 5) C. Kang, I. H. Maeng, S. J. Oh, J.-H. Son, T.-I. Jeon, K. H. An, S. C.

- Lim, and Y. H. Lee: *Appl. Phys. Lett.* **87** (2005) 041908.
- 6) V. K. Thorsmølle, R. D. Averitt, T. Shibauchi, M. F. Hundley, and A. J. Taylor: *Phys. Rev. Lett.* **97** (2006) 237001.
- 7) P. Y. Han, G. C. Cho, and X.-C. Zhang: *Opt. Lett.* **25** (2000) 242.
- 8) J. L. Johnson, T. D. Dorney, and D. M. Mittleman: *Appl. Phys. Lett.* **78** (2001) 835.
- 9) C. Ronne, P. Strand, and S. R. Keiding: *Phys. Rev. Lett.* **82** (1999) 2888.
- 10) M. Brucherseifer, M. Nagel, P. H. Bolivar, and H. Kurz: *Appl. Phys. Lett.* **77** (2000) 4049.
- 11) B. E. Cole, J. B. Williams, B. T. King, M. S. Sherwin, and C. R. Stanley: *Nature* **410** (2001) 60.
- 12) J. Ahn, D. N. Hutchinson, C. Rangan, and P. H. Buchsbaum: *Phys. Rev. Lett.* **86** (2001) 1179.
- 13) Y. Nakamura, Yu. A. Pashkin, and J. S. Tsai: *Nature* **398** (1999) 786.
- 14) C. Winnewisser, P. Uhd Jepsen, M. Schall, V. Schyja, and H. Helm: *Appl. Phys. Lett.* **70** (1997) 3069.
- 15) Q. Wu and X.-C. Zhang: *Appl. Phys. Lett.* **68** (1996) 1604.
- 16) Q. Wu and X.-C. Zhang: *Appl. Phys. Lett.* **71** (1997) 1285.
- 17) X. Xie, J. Xu, and X.-C. Zhang: *Opt. Lett.* **31** (2006) 978.
- 18) J. Ahn, A. Efimov, R. Averitt, and A. Taylor: *Opt. Express* **11** (2003) 2486.
- 19) H. S. Kang, F. G. Sun, T. K. Kim, and X.-C. Zhang: *Tech. Dig. CLEO-PR*, 1999, p. 1107.
- 20) K. Liu, H. S. Kang, T. K. Kim, and X.-C. Zhang: *Appl. Phys. Lett.* **81** (2002) 4115.
- 21) A. Nahata, A. S. Welington, and T. F. Heinz: *Appl. Phys. Lett.* **69** (1996) 2321.
- 22) J.-P. Caumes, L. Videau, C. Rouyer, and E. Freysz: *Phys. Rev. Lett.* **89** (2002) 047401.
- 23) M. I. Bell: *Phys. Rev. B* **6** (1972) 516.
- 24) T. Hattori, Y. Homma, A. Mitsuishi, and M. Tacke: *Opt. Commun.* **7** (1973) 229.
- 25) M. Schall, H. Helm, and S. R. Keiding: *Int. J. Infrared Millimeter Waves* **20** (1999) 595.
- 26) Y. R. Shen: *Principles of Nonlinear Optics* (Academic Press, New York, 1984) p. 42.
- 27) Q. Chen, M. Tani, Z. Jiang, and X.-C. Zhang: *J. Opt. Soc. Am. B* **18** (2001) 823.
- 28) D. T. F. Marple: *J. Appl. Phys.* **35** (1964) 539.